The Cryosphere Discuss., 6, 2715–2749, 2012
www.the-cryosphere-discuss.net/6/2715/2012/
doi:10.5194/tcd-6-2715-2012

The Cryosphere Discussions

Analysis of the snow-atmosphere energy balance during wet-snow instabilities and implications for avalanche prediction

C. Mitterer and J. Schweizer

WSL Institute for Snow and Avalanche Research SLF, Davos Dorf, Switzerland

Received: 14 June 2012 – Accepted: 3 July 2012 – Published: 23 July 2012

Correspondence to: C. Mitterer (mitterer@slf.ch)

Published by Copernicus Publications on behalf of the European Geosciences Union.

Abstract

Wet-snow avalanches are notoriously difficult to predict, as their formation mechanism is poorly understood and in-situ measurements closely related to instability are inexistent. Instead, air temperature is commonly used as predictor variable for days with high wet-snow avalanche danger – with limited success. As melt water is a major driver of wet-snow instability and snow melt depends on the energy input into the snow cover, we computed the energy balance and study whether it is a better proxy than meteorological parameters such as air temperature for predicting periods with high wet-snow avalanche activity. The energy balance was partly measured and partly modelled for virtual slopes at different elevations for the aspects south and north using the 1-D snow cover model SNOWPACK. We used measured meteorological variables and computed energy balance and its components to compare wet-snow avalanche days to non-avalanche days for four consecutive winter seasons in the surroundings of Davos, Switzerland. Air temperature, the net shortwave radiation and the energy input integrated over 3 or 5 days showed best results in discriminating event from non-event days. Multivariate statistics, however, revealed that for better predicting avalanche days, information on the cold content of the snowpack is necessary. Wet-snow avalanche activity was closely related to periods when large parts of the snowpack reached an isothermal state (0 °C) and energy input exceeded a maximum value of 200 kJ m^{-2} in one day, or the 3-day sum of positive energy input was larger than 1.2 MJ m^{-2}. Prediction accuracy with measured meteorological variables was as good as with computed energy balance parameters, but simulated energy balance variables accounted better for different aspects, slopes and elevations than meteorological data.

1 Introduction

Wet-snow avalanches are particularly difficult to forecast, but often threaten communication lines in snow-covered mountain areas. Once the snowpack becomes wet the

release probability obviously increases, but determining the peak and end of a period of high wet-snow avalanche activity is particularly difficult (Techel and Pielmeier, 2009).

Processes leading to wet-snow avalanches are complex and the conditions of the snowpack may change from stable to unstable in the range of hours (Trautman, 2008). The presence of liquid water within the snowpack in the starting zone is a prerequisite and several field campaigns (Brun and Rey, 1987; Bhutiyani, 1996) and experiments under laboratory conditions (Zwimpfer, 2011; Yamanoi and Endo, 2002) found decreasing shear strength with increasing liquid water content. However, quantifying the amount of liquid water within the snowpack is a difficult task as even experienced observers tend to overestimate the amount of liquid water (Fierz and Föhn, 1995; Techel and Pielmeier, 2011). Only objective measurement devices relating the relative permittivity of the 3-phase medium wet snow to an amount of water provide reliable results. Most devices though are for research purposes only and until today the operational use is hindered by practical and financial constraints. In addition, no established procedure exists to assess wet-snow instability. In-situ stability tests commonly used to assess dry-snow instability showed ambiguous results when performed in moist or wet snow covers (Techel and Pielmeier, 2010).

Given the poor understanding of the formation mechanism and the lack of indicative measurements, statistical rather than physical modelling has been used to predict wet-snow instability. While for large new snow avalanches the 3-day sum of precipitation is the strongest forecasting parameter (Schweizer et al., 2009) and closely related to avalanche danger (Schweizer et al., 2003a), air temperature is often used as a critical parameter for predicting wet-snow avalanche activity (McClung and Schaerer, 2006). It is included in statistical prediction tools which were designed for a defined climatic region (Romig et al., 2005). However, there are many examples which show that air temperature is in many cases not a good predictor and causes a high number of false alarms (Kattelmann, 1985). Nevertheless, it appears to be a variable clearly related to wet-snow instability (Baggi and Schweizer, 2009; Peitzsch et al., 2012).

To clarify the meteorological boundary conditions favouring the triggering of wet-snow avalanches, we analyzed four winter seasons (from 2007–2008 to 2010–2011) with different distinct wet-snow avalanche events in the surroundings of Davos, Switzerland. As suggested by Trautman (2008) we computed the entire energy balance for the snowpack with special attention to the main sources for snow melt, namely the incoming longwave and shortwave radiation and the sensible heat flux (Ohmura, 2001). We used univariate and multivariate statistics to evaluate whether those three sources were relevant shortly before and during the instabilities. In addition, we analyzed meteorological parameters of nearby stations and evaluated whether the energy balance and its terms performed better than widely used meteorological parameters such as air temperature.

2 Data

2.1 Avalanche occurrence

Avalanche occurrence data were recorded for the winters 2007–2008 to 2010–2011 for the surroundings of Davos, Switzerland. Data consisted of avalanche size (Canadian avalanche size class, McClung and Schaerer, 2006) and included only events which were classified as wet-snow avalanches. We calculated a daily avalanche activity index (AAI) using a weighted sum of recorded avalanches per day with weights of 0.01, 0.1, 1 and 10 for size classes 1 to 4, respectively (Schweizer et al., 2003b). For the statistical analyses (see below) only days with an AAI > 2 were considered as wet-snow avalanche days. In addition, we calculated the median elevation of the release zones. Due to the recording system used in Switzerland it was not possible to clearly relate avalanches and their size to a given aspect. Therefore we introduced an aspect index, which is the ratio of the frequency and size of avalanches recorded in southern aspects to the one recorded in northern aspects. If the ratio was >1 we assumed that the avalanche cycle took place in southern aspects and vice versa for <1. Following

this approach we obtained 66 wet-snow avalanche days and 663 non-avalanche days for the four winters. The major avalanche cycles with date, aspect index and elevation of release zones are given in Table 1.

2.2 Meteorological data

Meteorological data were obtained from three automatic weather stations: Weissfluhjoch (WFJ, 2540 m a.s.l.), Stillberg (STB, 2150 m) and Dorfberg (DFB, 2140 m). After the first winter season 2007–2008 data from STB were replaced by data from the new Dorfberg weather station which is located in the vicinity of a well-known wet-snow avalanche starting zone. The three stations are located at two distinct elevations: STB and DFB are slightly above the tree-line, near the lower limit of where most wet-slab avalanches are initiated, and WFJ is located higher than most starting zones of all wet-snow avalanche cycles.

For the statistical analyses radiation (all four components), snow depth, relative humidity and air temperature were used as explanatory variables. In addition to mean, maximum and minimum values we derived differences and sums over 1, 3 and 5 days; wind was not considered.

2.3 Simulations with SNOWPACK

In order to obtain energy balance data for slopes of various elevations and aspects we used the 1-D snow cover model SNOWPACK (Lehning et al., 2002a,b; Lehning and Fierz, 2008). Slope angle was fixed to 35° which represents the median slope angle of all recorded wet-snow avalanche releases. Input data for the model were meteorological values taken from the weather station Weissfluhjoch (WFJ) only; we had to extrapolate or adapt air temperature, snow surface temperature and incoming shortwave radiation for different elevations and aspects. Air temperature was extrapolated using a constant lapse rate of 0.65 °C/100 m. Outgoing longwave radiation and consequently snow surface temperature was modelled in SNOWPACK using Neumann

boundary conditions (Lehning et al., 2002b). We adapted the input of the shortwave radiation according to the lapse rate suggested by Marty (2001). We did simulations only for slopes of the two main aspects, i.e. 0° N and 180° S. The change in incoming solar radiation on these aspects was taken into account. Summarizing, we used air temperature, incoming shortwave, incoming longwave, reflected shortwave radiation, wind direction, wind speed, and snow depth to run the model. Components of the radiation balance and air temperature including relative humidity were measured under ventilated conditions. Simulations were performed for 2000, 2200 and 2500 m a.s.l. For slope simulations, snow depth was modelled with a precipitation mass input and albedo was determined as a function of grain type, grain size and presence of liquid water at the snow surface. Again daily means, maximum, minimum and 1, 3 and 5 day sums were derived from the energy balance terms.

3 Methods

3.1 Calculation of energy balance and liquid water

The energy balance was calculated using SNOWPACK. Within the model the energy balance can be calculated in two different ways. The first mode calculates the net change rate $\mathrm{d}H/\mathrm{d}t$ of the snowpack's internal energy per unit area as the sum of all energy fluxes at the surface:

$$-\frac{\mathrm{d}H}{\mathrm{d}t} = S^{\downarrow} + S^{\uparrow} + L^{\downarrow} + L^{\uparrow} + H_{\mathrm{S}} + H_{\mathrm{L}} + H_{\mathrm{P}} + G \quad (1)$$

where $S^{\downarrow}$ and $S^{\uparrow}$ are the downward and reflected components of shortwave radiation, respectively, $L^{\downarrow}$ and $L^{\uparrow}$ are the downward and upward components of longwave radiation, respectively, H_{S} and H_{L} are the turbulent fluxes of sensible and latent heat through the atmosphere, H_{P} is the flux of energy carried as sensible or latent heat by both precipitation and blowing snow, G is the ground heat flux (King et al., 2008).

For our analyses $S^{\downarrow}$, $S^{\uparrow}$, $L^{\downarrow}$ and $L^{\uparrow}$ were measured, H_S, H_L and H_P modelled, and G fixed to a constant value. The sensible heat H_S (Eq. 2) and the latent heat flux H_L (Eq. 4) were calculated assuming a neutral atmospheric surface layer and using Monin-Obukhov similarity theory resulting in:

$$H_S(0) = -C\rho_a c_p(T(z) - T(0)), \tag{2}$$

where $T(z)$ is the air temperature at height z, $T(0)$ the snow surface temperature, ρ_a the density of air and c_p the heat capacity; the kinematic transfer coefficient C is given according to:

$$C = \frac{-ku_*}{0.74 \ln \frac{z}{z_0}}, \tag{3}$$

where k is the von Karman constant, u_* is the friction velocity of the wind and z the height of the wind measurement. The latent heat is given as:

$$H_L = -C\frac{0.622L^{w/i}}{R_a T(z)}\left[e_s^w(T(z))\mathrm{RH} - e_s^i(T(0))\right], \tag{4}$$

where R_a is the gas constant for dry air, $L^{w/i}$ are the latent heat values for vaporization and sublimation, respectively, $e_s^{w/i}$ is the saturation vapour pressure over water or ice, and RH the relative humidity.

Assuming neutral stability conditions is valid during periods with moderate to high wind speeds which is often the case under complex terrain conditions (Lehning et al., 2002a). Stössel et al. (2010) showed that outgoing longwave radiation is better accounted for within SNOWPACK when forcing neutral conditions.

The second option in SNOWPACK is to calculate the internal change of energy based on either warming and melting, or cooling and freezing; it is given by:

$$-\frac{dH}{dt} = L_{li}(R_F - R_M) - \int_0^{HS}\left[\frac{d}{dt}\left(\rho_s(z)c_{p,i}T_s(z)\right)\right]dz, \tag{5}$$

where R_F and R_M are the freezing and melting rate, respectively, L_{li} the latent heat of fusion of ice, and $c_{p,i}$ the specific heat capacity of ice; ρ_s is the snow density and T_s is the snow temperature, both at height z (King et al., 2008). The second mode also allows for calculating the cold content of the snowpack, which is the integral over the snowpack depth HS, i.e. the second term of the RHS in Eq. (5). In other words, the cold content describes how much energy is needed to warm the snow to 0 °C. In this way it was possible to model whether the input energy resulting from the energy flux at the surface is used for warming or already for melting snow. A snowpack, where at every height z the cold content equals $0\,\mathrm{kJ\,m^{-2}}$, is equivalent to an isothermal snowpack. We calculated the proportion of the snowpack reaching this state and refer to it as proportion zero cold content.

SNOWPACK contains parameterisations of water percolation, retention and refreezing processes and calculates the liquid water content for single layers. There are two possibilities to calculate the liquid water content for every layer within the modelled snow cover (Hirashima et al., 2010). Since water transport, especially on slopes is a very complex phenomenon, the water transport codes that are presently implemented within SNOWPACK cannot depict the full complexity of flowing water within the snowpack which is responsible for wet-snow avalanche formation. Both approaches have benefits, but compared to observations substantial deviations were found (Mitterer et al., 2011). Therefore, we did not use liquid water values calculated for single layers with one of the two schemes in the statistical analyses. Instead we used the total amount of liquid water within the snowpack. This value is directly linked to the energy

balance and the cold content of snow and gives an estimate of how much water was present during the days with wet-snow avalanche activity.

3.2 Statistical analyses

The non-parametric Mann-Whitney *U*-test (Spiegel and Stephens, 1999) was used to contrast meteorological or energy flux variables from avalanche and non-avalanche days. Observed differences were judged to be statistically significant where the level of significance was $p < 0.05$, i.e. the null hypothesis that the two groups are from the same population was rejected. In order to match the monthly distribution of avalanche days, we randomly selected the same number of non-avalanche days considering the frequency of wet-snow avalanche days per month for the period December–May. Days with an AAI ≤ 2 were excluded as our focus is on prediction of a regional avalanche activity. Non-avalanche days were selected 10 times and for every run a *p*-value was computed. We averaged the *p*-values and only if the *U*-test indicated a statistically significant difference, variables were passed to a classification tree analysis (Breiman et al., 1998) and its newer derivative the RandomForest classification (Breiman, 2001). Classification trees were obtained by optimising the misclassification costs and the complexity (size) of a tree. Tree size was determined through cross-validation (10-fold). To minimize the effect of randomly selecting non-avalanche days we performed the tree analysis 20 times and selected the tree combination, which showed up in most of the cases (in our case about 2/3).

RandomForest (RF) is a newer derivative of the classification tree analysis. We used the package RandomForest (Version 4.6-2) incorporated in the R-project. The code is based on the work of Breiman (2001). It uses bootstrap samples to construct multiple trees. Each tree is grown with a randomized subset of predictors that allows the trees to grow to their maximum size without pruning. Finally the results of all trees are aggregated by averaging the trees. Out-of-bag samples are used to calculate an unbiased error rate and variable importance, without the need for a training data set or cross validation. Variable importance is based on how much worse the prediction would be

if the data for that predictor were permuted randomly. The stronger the decrease in prediction accuracy, the more important is the variable (Breiman, 2001). As this importance measure is calculated for each node, a more local importance is given. For our data set we produced $N = 500$ trees and restricted the randomized subset of predictors to a minimum of 7, but a maximum of $\sqrt{n}$, where n is the number of predictors passed from the results of the *U*-test. To assess the performance of the multivariate analysis (classification tree and RandomForest) we used the true skill statistic (HK), the false alarm ratio (FAR), the probabilities of detection of events (POD), and non-events (PON). With definitions used in contingency tables (Table 2) the measures are defined as follows (Wilks, 1995; Doswell et al., 1990):

$$\text{Probability of detection: POD} = \frac{d}{b+d} \tag{6}$$

$$\text{Probability of non-events: PON} = \frac{a}{a+c} \tag{7}$$

$$\text{False alarm ratio FAR} = \frac{c}{c+d} \tag{8}$$

$$\text{True skill statistic HK} = \frac{d}{b+d} - \frac{c}{a+c} \tag{9}$$

The true skill statistic, also called the Hanssen and Kuipers discriminant, is a measure of the forecast success and accounts for the correct discrimination of events and non-events. Of course, false-stable prediction can have more serious consequences than false alarms, but too many false alarms will not provide meaningful insight into the meteorological boundary conditions prevailing during wet-snow instabilities as we cannot define patterns which are common for unstable wet-snow situations.

4 Results

We first report on the univariate analysis of the data including the meteorological parameters (Table 3) and those obtained by calculating the energy balance (Table 4,

Fig. 1). Then we present the results obtained with the multivariate approaches, classification trees (Figs. 2, 4) and RandomForest (Fig. 3) and compare the predictive power of the models created with either meteorological measurements or energy balance variables (Tables 3 and 4).

4.1 Univariate analysis

For the meteorological variables minimum, mean, maximum, and the positive sum of air temperature over 3 days, the distributions were statistically different with $p < 0.01$ for the two classes of wet-snow avalanche day/non-avalanche day (Table 3). Therefore, these variables were significant indicators for a day with an AAI > 2. Furthermore, the distributions for the minimum snow surface temperature (T_{SS}) were significantly different between the two classes for all stations. The mean and maximum of T_{SS}, the difference of air temperature in the last 24 h and the difference in snow height for 24 h or 3 days discriminated between the groups only with the data of WFJ. Not surprisingly, days with an AAI > 2 had always higher air and snow surface temperatures and a preceding period (3 or 5 days) with higher air temperatures than non-avalanche days. Also significant differences between the two groups of days were found for some variables derived from the radiation balance measured at the stations. Avalanche days received more energy input through radiation than non-avalanche days, though not always significantly different; outgoing longwave radiation ($L^{\uparrow}$) showed always high values for avalanche days. In other words, T_{SS} was always higher on avalanche days than on non-avalanche days.

The daily minimum of sensible heat (H_S), the mean net longwave, the minimum, mean, maximum value of $L^{\uparrow}$, all sums of $L^{\uparrow}$ and the 3-day sum of positive energy balance were the only variables for which the differences were judged significant for both aspects (Table 4). All other variables appear only in one of the two aspect classes. For the simulations on south-facing slopes all variables dealing with net and incoming shortwave radiation ($S^{\downarrow}$) discriminated well between avalanche and non-event days. Daily minimum and maximum values of the energy balance performed well in

distinguishing between avalanche and non-avalanche days for southern slopes only. On wet-snow avalanche days on south-facing slopes, the energy input into the snowpack was higher due to high net shortwave radiation and higher net longwave radiation than on non-avalanche days. Avalanche days on north-facing slopes were characterized by a high minimum value of H_S and long periods (3 days) of energy input. $L^{\uparrow}$ was always higher on avalanche days than on non-avalanche days.

The maximum value for the total amount of liquid water within the snowpack discriminated well between avalanche and non-avalanche days, but only for southern aspects (Fig. 1a). The difference becomes even more evident when including all available non-avalanche days (Fig. 1b). The interquartile ranges of the two distributions do not overlap at all, however, a considerable number of outliers depict days whenever high amount of liquid water was present, but no activity was recorded. For north-facing slopes the two distributions were similar (Table 4).

4.2 Multivariate analysis

For the multivariate approaches we pre-selected the variables based on Tables 3 and 4 according to their physical meaningfulness and significance in the univariate approach. Again, the same quantity of non-avalanche days ($N = 66$) was selected according to the frequency of avalanche days ($N = 66$) for the months December–May.

The classification tree with the meteorological parameters of WFJ used only terms of the radiation balance to split into the two classes. Air temperature was not chosen by the tree (Fig. 2). Avalanche days were detected with almost 90 % accuracy when following the nodes of the tree; non-event days were identified with a probability of 80 %. False-stable predictions were less frequent than false alarms. The RandomForest (RF) model with the WFJ data included beside different radiation terms, the 3-day sum of positive air temperature and the maximum air temperature into the top-five important variables (Fig. 3c). Predictive performance of the RF statistical model was 10–20 % worse than the one of the classification tree. POD and PON decreased to 69 %, concurrently FAR increased to 34 %. In the tree compiled with the DFB data set (not shown

here), the sum of air temperature over 24 h and the values of relative humidity were the dominant splitting parameters. The RF could not be applied to the DFB data as the univariate analysis did not reveal enough variables ($N < 7$) that discriminated between the two groups of days. The model performance of the DFB tree was worse than the performance of the tree obtained with the WFJ data (Table 5). The DFB tree found the events with good accuracy, but produced more false alarms and scored low in detecting non-events.

For a south-facing slope at 2500 m a.s.l., the energy balance summed over 3 days split best followed by the mean net shortwave radiation using classification tree analysis (Fig. 4). The following nodes included the internal state of energy of the snowpack (zero cold content) and the maximum outgoing longwave radiation. For northern slopes (not shown here), again the sum of the energy balance over 3 days split best. The subsequent nodes included sensible heat and the mean of net longwave radiation. Results obtained with RandomForests are very similar to those from classification trees, but variable importance differed. Most important variable was the value of zero cold content at noon followed by the mean net shortwave radiation for southern aspects and the mean outgoing longwave radiation for northern aspects. Only then the sum of the positive energy balance values shows up for both aspects (Fig. 3a, b). Again the results obtained with the tree outperform the predictive skills of RF. In none of the multivariate approaches variables related to the total amount of liquid water were chosen.

In summary, for southern and northern slopes the energy balance over 3 days was the variable that split best between avalanche and non-avalanche days. The following splitting rules included incoming short wave radiation and state of the internal energy for southern slopes and the sensible and net longwave radiation flux for northern slopes. For all cases the predictive skills of the trees were better than the ones of the RF analysis.

4.3 Predictive skills of air temperature and energy balance

So far results showed that the predictive skills of the two approaches with various input data sets were rather good and mostly agreed. In a next step, however, we wanted to know if air temperature or the energy balance is sufficient for wet-snow avalanche forecasting and which of both performs better. When omitting the radiation terms in the tree presented in Fig. 2, the 5-day sum of positive air temperature remained as the only splitting parameter (Fig. 5a), but model performance deteriorated (Table 5): the tree missed two thirds of all avalanche events, but hardly missed any non-event days. False alarms (0.11) were fairly infrequent. When adding the snow surface temperature (Fig. 5b) the predictive power improved (POD = 0.89, PON = 0.6, FAR = 0.3), but the prediction accuracy for the non-events went down and the false-alarm ratio increased. Nevertheless the number of false-stable predictions was in the same range as with the more complex tree in Fig. 2. Using only information of the energy balance, the tree identified almost all events, but missed many non-events which means that almost 2/3 of all non-avalanche days were classified as avalanche days. Introducing the outgoing longwave radiation (not shown here) increased the probability of non-events to 90 %, but decreased the probability to hit an avalanche day to 67 %.

5 Discussion

Studying the melt of ice on glaciers, Ohmura (2001) has pointed out that air temperature is a reliable proxy for calculating the melt and that considering the full energy balance does not substantially improve the results. This simple method is debatable, but seems to work for glaciological studies. One might therefore conclude that the same approach might work for predicting wet-snow avalanches as melting water is closely related to snowpack instability. On glaciers most melting is taking place during late spring and summer, when high air temperatures and a low albedo have an increasing effect on energy balance. The recorded wet-snow avalanches occurred in spring on steep

terrain (in our case the median slope angle is around 35°) and therefore conditions and the contribution of the different energy balance terms are different from the ablation zones and period on glaciers.

As most cycles in the periods we analysed occurred on slopes of southern aspect, it is not surprising that the net shortwave radiation provides most energy (Fig. 6). As single parameter it discriminated between event and non-event days for steep (=35°) southern aspects. Median values on avalanche days were about 80 W m^{-2}, however, maximum values may be as high as 200–400 W m^{-2} within 60 min (Fig. 6). These maximum flux values might prevail only for 2–4 h per day, but cover around two thirds of the maximum energy input of a single day (Table 4). In case the snowpack is already at 0 °C, this high energy input during a few hours will be directly transformed into ∼1.5 mm of water. As the correct calculation of the net shortwave radiation for virtual slopes is highly dependent on terrain properties and their position to the sun, it is very important to use the terrain information of the release area during the simulation. It might be possible to better account for those differences using a distributed energy balance model such as e.g. ALPINE3D (Lehning et al., 2006). In this way subtle changes in slope angle or aspect can be included. This approach might be suited to better predict periods of high avalanche probability and hence be used as tool in avalanche warning in future, but has at the moment severe computational limitations.

During the analysed periods incoming longwave radiation was the largest energy source, though always exceeded by the outgoing longwave radiation. In fact, the mean net longwave radiation was in general the largest negative component, i.e. energy loss (Fig. 6). It seems, however, decisive how negative this sink was. Low negative values hint to days with cloud cover or a melting snow surface. Cloud cover will attenuate the cooling effect at the snow surface, which will lead to a high value for $L^{\uparrow}$. In fact, $L^{\uparrow}$ was in all statistical models a good splitting parameter and appears to be very important whenever this parameter shows high values (Table 4; Fig. 3). High $L^{\uparrow}$ values correspond to a snow surface temperature close or at its melting point providing the

possibility to estimate whether the surplus of energy is used for warming or already for melting snow.

The values of the turbulent heat fluxes (H_S and H_L) were in general lower than half the magnitude of the net irradiative fluxes, but especially H_S may on some days early in spring exceed the magnitude of the irradiative terms and therefore needs to be considered when calculating the energy input to the snowpack on a daily basis. It is, however, very difficult to asses H_S precisely for large regions. The bulk method, which is used within SNOWPACK to calculate the turbulent fluxes, is at best an estimate. It has, however, been shown that the method gives robust results for the location of the recorded weather data, in our case the station Weissfluhjoch and the simulations for 2500 m a.s.l. (Plüss and Mazzoni, 1994). In order to obtain good results for the locations where the input needs to be extrapolated, air temperature, snow surface temperature and wind speed have to be representative. None of the three parameters can be verified for the slope simulations. Comparing the measured air temperature at the station Weissfluhjoch (2540 m a.s.l.) to the one at the station Dorfberg suggests that the average lapse rate may be some higher than the standard lapse rate of 0.65 °C/100 m. This means that we underestimate the mean H_S already due to our assumed lapse rate by 5 W m^{-2} for an elevation of 2200 m. Considering in addition the fact that the bulk method generally underestimates the sensible heat flux (Arck and Scherer, 2002), the presented values of H_S may well underestimate the sensible heat flux. A distributed modelling approach may help to assess the uncertainties.

Values of H_L seem to be of minor importance. Relative humidity, however, was a significant splitter in the univariate analysis. In fact, for the tree built with data of the station Dorfberg, relative humidity was used again (with higher values for avalanche days than non-avalanche days). This might suggest that fluxes of H_L were less negative or even towards the snowpack. The findings agree also with the fact that the incoming longwave radiation tended to be always higher on event days than non-event days, but are contradictory to previous results (Peitzsch et al., 2012).

It was not possible to introduce modelled melt water values within the analysis as the shortcomings of reproducing the movement of water within snow are too large or not well understood (Mitterer et al., 2011). The total amount of liquid water, was closely related to days with wet-snow avalanche occurrence on southern slopes. This value, though, rather gives information on the energy balance and the thermal state of the snowpack integrated over an extended period than reproducing the exact amount of water retained at the position of simulation. Figure 7 shows the total amount of liquid water and the proportion of zero cold content for two different elevations during the spring of 2009. Prevailing high amounts of water production and a high proportion of zero cold content after the major avalanche cycle hampers the application of this variable for prediction as too many non-avalanche days show the same behaviour and have a high production of water. In fact, none of the multivariate approaches used the total amount of water as a variable in its splitting rules.

Cold content seems to be more indicative for wet-snow instabilities. The reason for that might be that during periods when parts of the snowpack are isothermal and water is produced, it percolates quickly through preferential flow paths. Water flow within the snowpack is reported to be often in the unstable flow regime, i.e. a uniform advance of percolating water with a shock-wave like progression can no longer be assumed. At the leading edge of the wetting front and/or at capillary or hydraulic barriers flow fingers will develop in which water will preferentially drain. Finger flow is probably most important at the beginning of the melt season, when it can reach potential weak layers rapidly. The advance of the finger front can be quite fast and ranges from 0.1 up to 1 $cm\,s^{-1}$ (Waldner et al., 2004). Depending on the diameter and the spatial distribution of the flow fingers, a short period of high energy input is providing a considerable amount of water that will penetrate deep into the snowpack. Variations in snow stratigraphy will speed up or slow down this process depending on the layering and the various properties of the snow layers. Once the snowpack is isothermal for some time, snow stratigraphy becomes more uniform. Consequently, water flow in snow will be more homogeneous and thus the effect of melt water percolation on snow stability becomes

less accidental. In other words, with a similar amount of energy input similar changes in snowpack stability can be expected. The fact, that the avalanche activity tended to be wide-spread and occurred within a few days suggests that snow stratigraphy was fairly uniform throughout the area – underlining the above assumption. On the other hand, though, the local snow stratigraphy and thus the mechanical interaction with water will still be decisive for single wet-snow avalanche events. Deeper lying interfaces prone to back up water through capillary or hydraulic barriers will affect stability. Those deep layers will loose their strength with increasing liquid water content (Yamanoi and Endo, 2002); they carry the more load the deeper they are within the snowpack. The unstable flow regime will be dominant until the snowpack is ripe (second half of April in Fig. 7). A drainage system might be established and water will no longer tend to be ponded and thus no longer affect stability (Kattelmann, 1985).

Our data included only one rain-on-snow event and the above-discussed results may be biased to situations where irradiation and air temperature caused the melting. Rain is very efficient in bringing large amounts of water into the snowpack and thereby promoting instability. Such rain-on-snow events often follow snow fall, thus snow stability may already be close to critical. Wet-snow avalanche activity therefore follows only a few hours after the rain fall event started (Conway and Raymond, 1993).

Using simply the daily energy balance allowed detecting 90 % of the wet-snow avalanche days; therefore energy balance is superior to air temperature in detecting events. The problem, however, is that many false alarms resulted which is not satisfying and lowers the overall predictive skill. The true skill statistic (HK) of the energy balance was similar to the one of air temperature. Air temperature solely is not suited for predicting the events, but detects non-events fairly good. Combining air temperature with snow surface temperature, both commonly measured parameters, improved predictive skills (Fig. 5).

Finally, the results suggest that no single variable describing the energy input is sufficient for forecasting wet-snow instability. Further, information on snow temperature and how this temperature is evolving over time is necessary. Having this additional

information we can exclude days when the energy input is used for warming the snowpack or determine when surplus of energy is used to melt snow. The findings are linked to previous results by Baggi and Schweizer (2009) and some avalanche warning services, e.g. in New Zealand (Conway, 2005), take this fact into account by relating the convergence of snow temperature at different heights towards 0 °C to the start of a period with high probability of wet-snow avalanche release.

6 Conclusions

We compared 4 yr of wet-snow avalanche occurrence in the surroundings of Davos, Switzerland to meteorological data measured by three automated weather stations and to simulated energy balance values. The energy balance was modelled for virtual slopes of south-facing and north-facing aspects using the 1-D snow cover model SNOWPACK. Univariate analyses revealed that the distributions of air temperature, its positive sum over 3 or 5 days, the snow surface temperature, the 3-day sum of positive energy balance, the daily maximum amount of liquid water within the snowpack and the minimum value of the sensible flux were statistically different for wet-snow avalanche and non-avalanche days suggesting that these variables have predictive power. Using only one variable for a forecast revealed low scores in predicting a day with high wet-snow avalanche activity. Too many false-alarms deteriorate the predictive power.

Combining various variables in two different multivariate approaches provided satisfactory results and is promising in predicting wet-snow avalanche days. The results obtained with the energy balance did not outperform those obtained with meteorological parameters. Nevertheless, the modelling of the energy balance for virtual slopes allows to simulate the energy input, state of energy of the snowpack (i.e. cold content) and total amount of water for specific slopes and aspects. Results suggest that for cycles when irradiation and air temperature dominate melting, the knowledge of the energy input and the state of energy of the snowpack are essential to improve predictive accuracy.

As net shortwave radiation was the major energy source in the cycles we described, it is suggested to include geometry of the terrain (elevation, aspect, slope angle) in a next step. Distributed modelling of the energy balance shall be compared to well-mapped avalanche occurrence data. For this purpose starting zone characteristics of wet-snow avalanches need to be recorded with high temporal and spatial resolution.

Acknowledgement. C.M. was funded by the Swiss National Science Foundation (SNF, grant 200021-126889). We thank C. Fierz who helped to setup the SNOWPACK simulations and programmed the possibility to deduce the change in cold content within the software. For stimulating discussions we are grateful to F. Techel, B. Reuter, M. Schirmer and M. Lehning. We would like to thank the numerous observers who collected the avalanche occurrence data.

References

Arck, M. and Scherer, D.: Problems in the determination of sensible heat flux over snow, Geogr. Ann. A, 84A, 157–169, 2002.

Baggi, S. and Schweizer, J.: Characteristics of wet snow avalanche activity: 20 years of observations from a high alpine valley (Dischma, Switzerland), Nat. Hazards, 50, 97–108, 2009.

Bhutiyani, M. R.: Field investigations on meltwater percolation and its effect on shear strength of wet snow, in: Proceedings of the International Symposium on Snow and Related Manifestations, edited by: Agrawal, K. C., 26–28 September 1994, Manali, India, Snow and Avalanche Study Establishment, Manali, India, 200–206, 1996.

Breiman, L.: Random forest, Mach. Learn., 45, 5–32, 2001.

Breiman, L., Friedman, J. H., Olshen, R. A., and Stone, C. J.: Classification and regression trees, CRC Press, Boca Raton, USA, 368 pp., 1998.

Brun, E. and Rey, C.: Field study on snow mechanical properties with special regard to liquid water content, IAHS-AISH P., 162, 183–193, 1987.

Conway, H.: Storm Lewis: a rain-on-snow event on the Milford Road, New Zealand, in: Proceedings, ISSW, 2004 International Snow Science Workshop, Jackson Hole WY, USA, 19–24 September 2004, 557–564, 2005.

Conway, H. and Raymond, C. F.: Snow stability during rain, J. Glaciol., 39, 635–642, 1993.

Doswell, A., Davies-Jones, R., and Keller, D.: On summary measures of skill in rare event forecasting based on contingency tables, Weather Forecast., 5, 576–585, 1990.
Fierz, C. and Föhn, P. M. B.: Long-term observation of the water content of an alpine snowpack, in: Proceedings International Snow Science Workshop, Snowbird, Utah, USA, 30 October–3 November 1994, 117–131, 1995.
Hirashima, H., Nishimura, K., Yamaguchi, S., Sato, A., and Lehning, M.: Numerical modeling of liquid water movement through layered snow based on new measurements of the water retention curve, Cold Reg. Sci. Technol., 64, 94–103, 2010.
Kattelmann, R.: Wet slab instability, in: Proceedings International Snow Science Workshop, Aspen, Colorado, USA, 24–27 October 1984, 102–108, 1985.
King, J. C., Pomeroy, J., Gray, D. M., Fierz, C., Föhn, P., Harding, R. J., Jordan, R., Martin, E., and Plüss, C.: Snow-atmposphere energy mass balance, in: Snow and Climate, edited by: Armstrong, R. and Brun, E., Cambridge University Press, Cambridge, 70–124, 2008.
Lehning, M. and Fierz, C.: Assessment of snow transport in avalanche terrain, Cold Reg. Sci. Technol., 51, 240–252, 2008.
Lehning, M., Bartelt, P., Brown, R. L., and Fierz, C.: A physical SNOWPACK model for the Swiss avalanche warning; Part III: meteorological forcing, thin layer formation and evaluation, Cold Reg. Sci. Technol., 35, 169–184, 2002a.
Lehning, M., Bartelt, P., Brown, R. L., Fierz, C., and Satyawali, P. K.: A physical SNOWPACK model for the Swiss avalanche warning; Part II: Snow microstructure, Cold Reg. Sci. Technol., 35, 147–167, 2002b.
Lehning, M., Völksch, I., Gustafsson, D., Nguyen, T., Stähli, M., and Zappa, M.: ALPINE3D: a detailed model of mountain surface processes and its application to snow hydrology, Hydrol. Process., 20, 2111–2128, 2006.
Marty, C.: Surface radiation, cloud forcing and greenhous effect in the Alps, Zürcher Klima-Schriften, Institut für Klimaforschung ETH, Zürich, Switzerland, 79, 122, 2001.
McClung, D. M. and Schaerer, P.: The Avalanche Handbook, 3rd edn., The Mountaineers Books, Seattle WA, USA, 342 pp., 2006.
Mitterer, C., Hirashima, H., and Schweizer, J.: Wet-snow instabilities: comparison of measured and modelled liquid water content and snow stratigraphy, Ann. Glaciol., 52, 201–208, 2011.
Ohmura, A.: Physical basis for the temperature-based melt-index method, J. Appl. Meteorol., 40, 753–761, 2001.

Peitzsch, E. H., Hendrikx, J., Fagre, D. B., and Reardon, B.: Examining spring wet slab and glide avalanche occurrence along the Going-to-the-Sun Road corridor, Glacier National Park, Montana, USA, Cold Reg. Sci. Technol., 78, 73–81, 2012.
Plüss, C. and Mazzoni, R.: The role of turbulent heat fluxes in energy balance of high alpine snow cover, Nord. Hydrol., 25, 25–38, 1994.
Romig, J. M., Custer, S. G., Birkeland, K. W., and Locke, W. W.: March wet avalanche prediction at Bridger Bowl Ski Area, Montana, in: Proceedings ISSW, 2004 International Snow Science Workshop, Jackson Hole WY, USA, 19–24 September 2004, 598–607, 2005.
Schweizer, J., Jamieson, J. B., and Schneebeli, M.: Snow avalanche formation, Rev. Geophys., 41, 1016, doi:10.1029/2002RG000123, 2003a.
Schweizer, J., Kronholm, K., and Wiesinger, T.: Verification of regional snowpack stability and avalanche danger, Cold Reg. Sci. Technol., 37, 277–288, 2003b.
Schweizer, J., Mitterer, C., and Stoffel, L.: On forecasting large and infrequent snow avalanches, Cold Reg. Sci. Technol., 59, 234–241, 2009.
Spiegel, M. R. and Stephens, L. J.: Schaum's outline of theory and problems of statistics, 3rd edn., Schaum's outline series, McGraw-Hill, New York, 538 pp., 1999.
Stössel, F., Guala, M., Fierz, C., Manes, C., and Lehning, M.: Micrometeorological and morphological observations of surface hoar dynamics on a mountain snow cover, Water Resour. Res., 46, W04511, doi:10.1029/2009WR008198, 2010.
Techel, F. and Pielmeier, C.: Wet snow diurnal evolution and stability assessment, in: Proceedings ISSW 2009, International Snow Science Workshop, Davos, Switzerland, 27 September–2 October 2009, 256–261, 2009.
Techel, F. and Pielmeier, C.: Snowpack properties of unstable wet snow slopes: observations from the Swiss Alps, in: Proceedings ISSW 2010, International Snow Science Workshop, Lake Tahoe, California, USA, 17–22 October 2010, 187–193, 2010.
Techel, F. and Pielmeier, C.: Point observations of liquid water content in wet snow – investigating methodical, spatial and temporal aspects, The Cryosphere, 5, 405–418, doi:10.5194/tc-5-405-2011, 2011.
Trautman, S.: Investigations into wet snow, The Avalanche Review, 26, 16–17, 2008.
Waldner, P., Schneebeli, M., Schultze-Zimmerman, U., and Flühler, H.: Effect of snow structure on water flow and solute transport, Hydrol. Process., 18, 1271–1290, 2004.
Wilks, D. S.: Statistical methods in the atmospheric sciences: an introduction, International Geophysics, Academic Press, San Diego CA, USA, 467 pp., 1995.

Yamanoi, K. and Endo, Y.: Dependence of shear strength of snow cover on density and water content, Seppyo J. Jpn. Soc. Snow Ice, 64, 443–451, 2002.
Zwimpfer, F.: Failure of wet snow, BSc Thesis, Swiss Federal Institute of Technology, Zurich, 45 pp., 2011.

Table 1. Major wet-snow avalanche cycles in the surroundings of Davos, Switzerland, for the winters 2007–2008 to 2010–2011. Aspect index was calculated by relating the number and size of avalanches released on slopes of northern to those on southern aspects. Only for the cycle on 23 April 2008 no clear aspect could be assigned.

Winter	Date	Aspect index	Median elevation of starting zones (m a.s.l.)
2007–2008	19 Apr	South	2400
	23 Apr	South/North	2250
2008–2009	18 Mar	South	2075
	1–8 Mar	South	2400
	28 Apr	South	2500
2009–2010	20–23 Mar	South	2400
2010–2011	1–2 Apr	South	2400
	6–8 Apr	North	2300

Table 2. Contingency table (total cases: $N = a + b + c + d$).

		Observed Non-avalanche day	Avalanche day
Model	Non-avalanche day	a: correct non-event	b: missed event
	Avalanche day	c: false alarm	d: correct event

Table 3. Comparison of avalanche (AvD) to non-avalanche days (nAvD) for meteorological data measured at the weather stations Weissfluhjoch (2540 m a.s.l.) and Dorfberg (2140 m a.s.l.). Median values are shown; Dorfberg values for the season 2007–2008 are substituted with values from Stillberg (2150 m a.s.l.). For each variable, distributions from avalanche days and non-avalanche days were contrasted (U-test), and the level of significance (p-value) is given. Only variables with $p < 0.05$ are shown.

Variable	Weissfluhjoch (WFJ) Median		p-value	Dorfberg (DFB) Median		p-value
	AvD	nAvD		AvD	nAvD	
TA_{mean} (°C)	−0.4	−4.1	<0.01	3.7	2.6	<0.01
TA_{min} (°C)	−2.3	−6.7	<0.01	0.5	−6.3	<0.01
TA_{max} (°C)	2.1	−1.5	<0.01	5.1	−0.7	<0.01
ΔTA3d (°C)	1.2	−0.1	0.01	1.2	0.1	0.42
Σ3d TA positive (°C)	65	4	<0.01	357	12	<0.01
Σ5d TA positive (°C)	97.3	15.7	0.01	520	54	0.01
ΔHS3d (cm)	−6	0	0.03	−1.5	0	0.36
TSS_{mean} (°C)	−4.2	−6.5	0.01	0	−4.2	0.04
TSS_{min} (°C)	−10.5	−13.2	0.04	−2.2	−11.6	<0.01
TSS_{max} (°C)	0	−1.6	<0.01	0	0	0.19
RH_{mean} (%)	69	78	0.09	72	69	0.03
Min radiation balance ($W m^{-2}$)	−77	−71	0.02	−72	−70	0.26
Max radiation balance ($W m^{-2}$)	110	69	0.04	501	241	0.26
Σ5d positive radiation balance ($W m^{-2}$)	3907	3354	0.7	17847	12582	0.49
Mean incoming shortwave ($W m^{-2}$)	227	204	0.02	215	173	0.2
Mean outgoing longwave ($W m^{-2}$)	301	291	0.02	315	297	0.03
Min outgoing longwave ($W m^{-2}$)	277	266	0.03	305	268	<0.01
Max outgoing longwave ($W m^{-2}$)	312	304	<0.01	NA	NA	–

Table 4. Comparison of avalanche (AvD) to non-avalanche days (nAvD) for variables derived from the energy balance calculated for a 35° slope. For each variable, distributions from avalanche days and non-avalanche days are contrasted (*U*-test), and the level of significance (*p*-value) is given. Only variables with $p < 0.05$ are shown.

Variable	Median for 2500 m, South		*p*-value	Median for 2500 m, North		*p*-value
	AvD	nAvD		AvD	nAvD	
Min sensible heat ($W m^{-2}$)	−5	−20	<0.01	3	−2	0.04
Mean net longwave ($W m^{-2}$)	−51	−35	0.02	−42	−31	0.02
Mean outgoing longwave ($W m^{-2}$)	302	293	<0.01	292	284	0.03
Min outgoing longwave ($W m^{-2}$)	277	267	0.03	270	261	0.04
Max outgoing longwave ($W m^{-2}$)	315	315	0.02	311	301	<0.01
Mean net shortwave ($kJ m^{-2}$)	72	52	0.01	19	17	0.35
Max net shortwave ($kJ m^{-2}$)	283	208	0.01	60	58	0.47
Mean incoming shortwave ($W m^{-2}$)	294	253	0.04	123	127	0.72
Mean energy balance ($kJ m^{-2}$)	16	2	0.01	2	1	0.12
Min energy balance ($kJ m^{-2}$)	−36	−79	<0.01	−16	−17	0.31
Max energy balance ($kJ m^{-2}$)	172	84	<0.01	20	17	0.22
Σ3d energy balance positive ($kJ m^{-2}$)	4356	1959	<0.01	671	493	<0.01
Σ5d energy balance positive ($kJ m^{-2}$)	6088	3840	0.14	1050	844	0.03
Proportion zero cold content at 12:00 h (%)	91	85	0.04	91	78	0.02
Max amount of total liquid water within the snowpack ($kg m^{-2}$)	23	9	<0.01	0	0	0.6

Table 5. Classification accuracy of different tree and RandomForest (RF) models for contrasting wet-snow avalanche days to non-avalanche days.

Model/Input	Probability of detection (POD)	Probability of non-events (PON)	False alarm ratio (FAR)	True skill score (HK)
Tree meteo data WFJ	0.89	0.8	0.18	0.7
Tree meteo data WFJ, T_A only	0.35	0.95	0.11	0.3
Tree meteo data WFJ, T_A+T_{SS}	0.89	0.6	0.3	0.5
Tree meteo data DFB	0.9	0.63	0.3	0.53
Tree energy balance 2500 m, S	0.77	0.92	0.08	0.7
Tree energy balance 2500 m, N	0.74	0.95	0.05	0.7
Tree energy balance only 2500 m, S	0.9	0.4	0.39	0.33
Tree energy balance and outgoing longwave 2500 m, S	0.67	0.94	0.08	0.61
RF meteo data WFJ	0.69	0.69	0.34	0.39
RF energy balance 2500 m, S	0.69	0.79	0.32	0.4
RF energy balance 2500 m, N	0.6	0.72	0.47	0.33

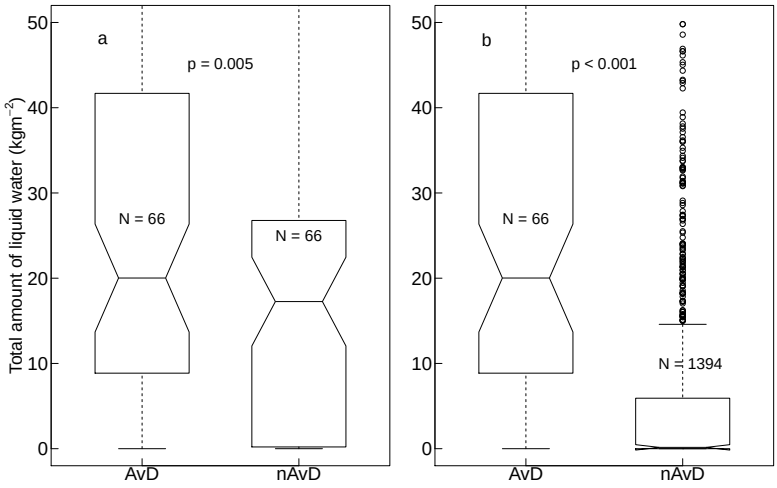

Fig. 1. Contrasting avalanche days (AvD) to non-avalanche days (nAvD) for the daily maximum amount of liquid water within the snowpack for **(a)** a subset of non-avalanche days and **(b)** all non-event days within the data set with data obtained from a simulation representing a south-facing slope. Boxes span the interquartile range, whisker extend to 1.5 times the interquartile range. Outliers are shown with open circles. Notches are defined by ±1.5 times the interquartile range divided by the square-root of *N*.

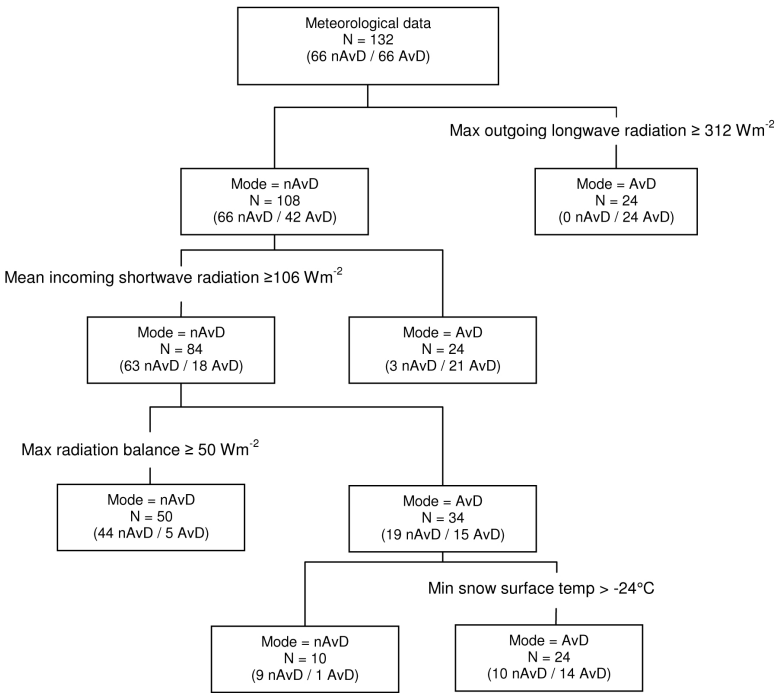

Fig. 2. Classification tree to discriminate between avalanche (AAI > 2) and non-avalanche days. Input data were all meteorological variables taken from WFJ if *U*-test was significant. Forecast scores of the tree: probability of detection (POD) = 0.89; probability of non-events (PON) = 0.8; true skill score (HK) = 0.69.

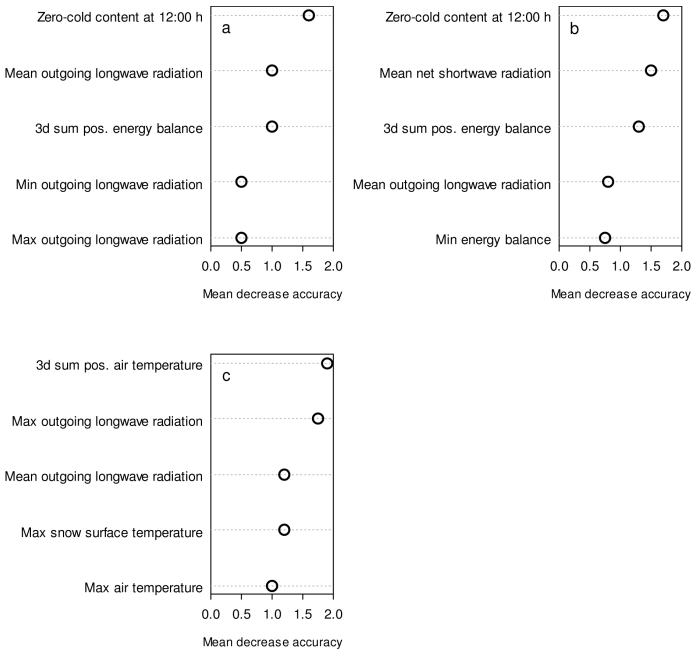

Fig. 3. The five most important variables for RandomForest models built with data obtained from **(a)** simulated northern slopes (2500 m, 35°), **(b)** simulated southern slopes (2500 m, 35°), and **(c)** meteorological parameters recorded at the station Weissfluhjoch to classify wet-snow avalanche and non-avalanche days. Variable importance is based on how much worse the prediction would be if the data for that predictor were permuted randomly; the stronger the decrease in accuracy, the higher is the variable importance.

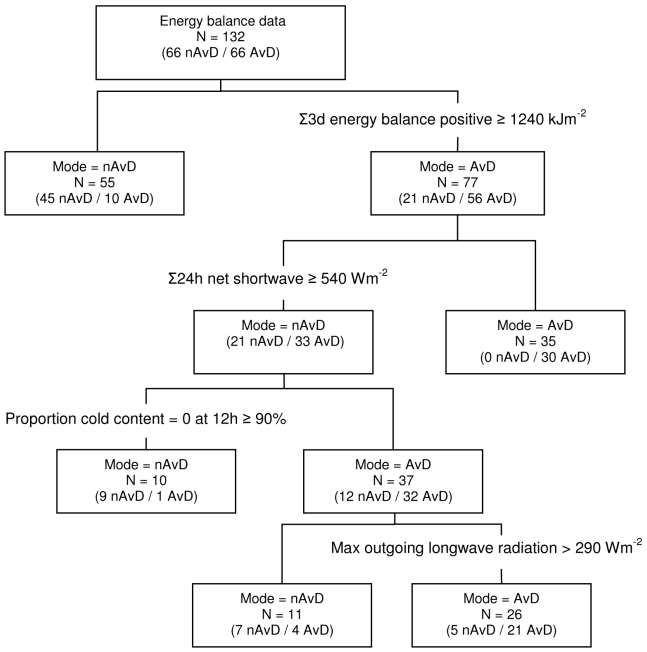

Fig. 4. Classification tree to discriminate between avalanche (AAI > 2) and non-avalanche days. Input data were all energy balance variables calculated for a 35° south-facing slope at 2500 m a.s.l. Forecast scores of the tree: probability of detection (POD) = 0.84; probability of non-events (PON) = 0.83; true skill score (HK) = 0.72.

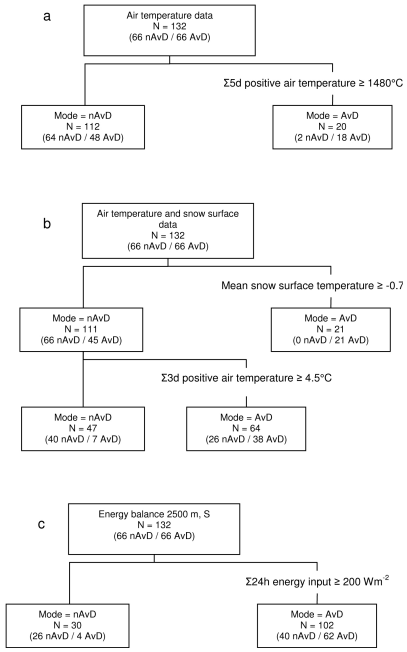

Fig. 5. (a) Classification tree for WFJ using air temperature information, **(b)** classification tree for air temperature and snow surface information and **(c)** for a virtual south-facing slope with energy balance information only (for predictive skills see Table 5).

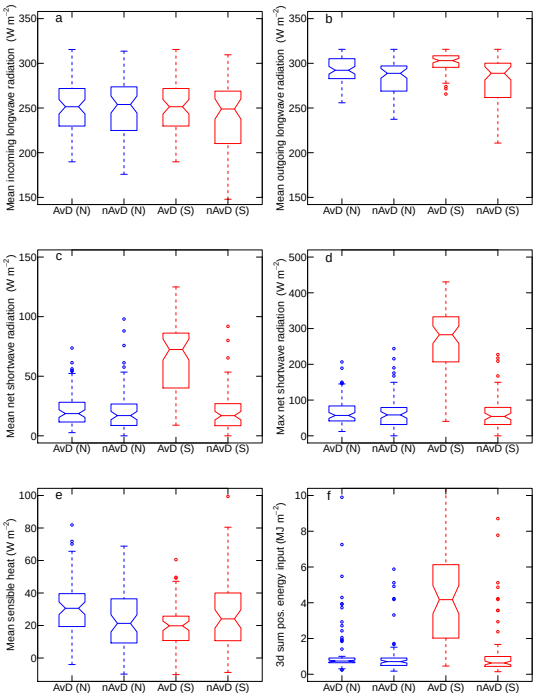

Fig. 6. Distribution of **(a)** mean incoming longwave radiation, **(b)** mean outgoing longwave radiation **(c)** mean net shortwave radiation, **(d)** max net shortwave radiation **(e)** mean sensible flux, and **(f)** the resulting 3-day sum of positive energy balance values for avalanche days (AvD) and non-avalanche days (nAvD) on south-facing (red) and north-facing (blue) slopes. Values were calculated with SNOWPACK assuming an elevation of 2500 m and a slope angle of 35°.

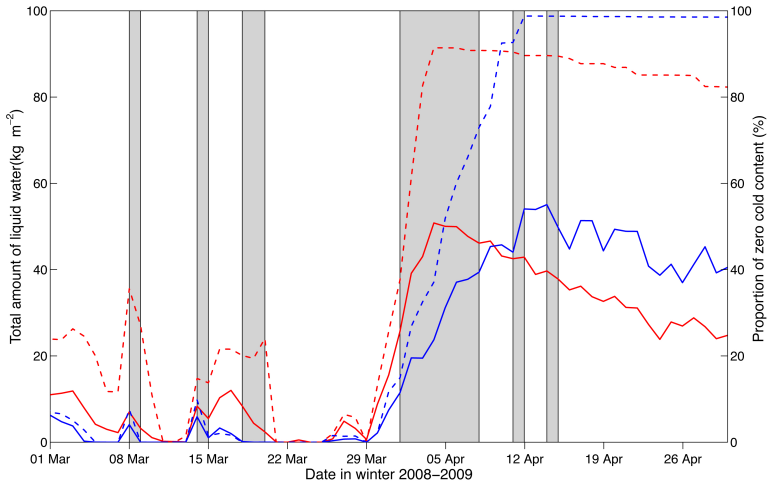

Fig. 7. Daily maximum amount of liquid water within the snowpack for a south-facing 35° slope at 2200 m a.s.l. (red solid line) and 2500 m a.s.l. (blue solid line). Dashed lines show the proportion of snowpack with a zero cold content (red = 2200 m; blue = 2500 m). The grey boxes indicate periods with wet-snow avalanche activity (AAI > 2) recorded for the surroundings of Davos, Switzerland.